metals

MDPI

Article

Phase and Morphology Transformations in Sulfur-Fixing and Reduction Roasting of Antimony Sulfide

Zhen Ouyang [1], Longgang Ye [1,*], Chaobo Tang [2] and Yifeng Chen [1]

[1] College of Metallurgy and Material Engineering, Hunan University of Technology, Zhuzhou 412007, China; oyz1032168134@163.com (Z.O.); happy610@126.com (Y.C.)

[2] School of Metallurgy and Environment, Central South University, Changsha 410083, China; tangchaobo9043@163.com

* Correspondence: 15388017911@163.com; Tel./Fax: +86-0731-2218-3453

Received: 1 January 2019; Accepted: 11 January 2019; Published: 14 January 2019

Abstract: Metallurgical extraction of antimony (Sb) currently has the limitations of high energy consumption and adverse environmental impact. In this study, we proposed a cleaning process to extract Sb by metallurgy and beneficiation based on S-fixing and reduction roasting of Sb_2S_3. Metallic Sb can be obtained directly by using zinc oxide (ZnO) and carbon as sulfur-fixing and reducing agents, respectively, at 600–1000 °C, wherein S is fixed in the form of ZnS. The thermodynamic feasibility of the process of roasting and the effects of a range of process parameters on Sb generation were investigated comprehensively. The optimum conditions for metallic Sb generation were determined to be as follows: temperature of 800 °C, C powder size of 100–150 mesh, ZnO content of 1.1 times its stoichiometric requirement (α), and reaction time of 2 h. Under the optimum conditions, the proportion of Sb distributed in the metal phase reached 90.44% and the S-fixing rate reached 94.86%. The phase transformation of Sb progressed as follows: $Sb_2S_3 \rightarrow Sb_2O_3 \rightarrow Sb$. The Sb particle had mainly spherical and hexahedral morphologies after quenching and furnace cooling, and bonded little with ZnS. This research is potentially beneficial for the further design process of Sb powder and ZnS recovery by mineral separation.

Keywords: antimony metallurgy; stibnite; zinc oxide; sulfur-fixing; roasting

1. Introduction

Antimony is a critical basic material, widely used in the manufacture of flame retardants, alloys, brake pads, and catalysts [1]. In 2014, the European Commission designated Sb as a critical raw material [2]. The ores from which Sb can be economically extracted are typically sulfides such as stibnite (Sb_2S_3) and jamesonite ($Pb_4FeSb_6S_{14}$), and these are distributed across China, Bolivia, Burma, Russia, and Tajikistan [3]. The pyrometallurgical process, involving oxidative volatilisation (>1200 °C) and reduction smelting (>1000 °C) at high temperatures, carried out in blast furnaces and reverberatory furnaces, respectively, has been the primary method of Sb extraction and accounts for more than 90% of the total Sb output [4]. The significant shortcomings of this method are high energy consumption (>3.6 × 10^{10} J/t Sb), large generation of low-concentration SO_2 [5], and risk of occupational disease due to volatilisation of As and Sb [6,7].

To improve the operational environment, researchers have developed several processes of intensified smelting, such as O_2-enriched smelting [8,9], molten salt smelting [10,11], and sulfur-fixing smelting [12]. In O_2-enriched smelting, O_2-enriched air is used to oxidise Sb_2S_3 concentrate to obtain high-concentration SO_2. This practice indicates that Sb_2O_3 coheres on the gas duct and exhibits a low melting point and bondability. We developed a process of reduction-matting-smelting to directly produce Sb at between 1000 °C and 1300 °C, and found that the direct recovery rate of Sb was low

for its volatilisation to proceed. Padilla et al. investigated S-fixing roasting of Sb_2S_3 using lime as a desulfurisation agent in the temperature range 700–850 °C [13,14]. This method showed potential for application in Sb extraction at low temperature with SO_2-free emission. However, it is difficult to dispose of CaS, the product of the S-fixing reaction, which is yet another hazardous solid waste.

Industrial hydrometallurgical practices can be divided into acidic and alkaline processes based on the leaching agents employed. In the acidic method, $FeCl_3/SbCl_5$-HCl mixture is used as the leaching solution and membrane electrowinning is subsequently conducted to extract Sb and regenerate the leaching reagent [15,16]. The main issues of this method are equipment corrosion by Cl, and hyperplasia of Fe^{2+} ions. In the alkaline method, the Na_2S-NaOH system is used as the leaching solution [17,18]. The obvious shortcoming of this method is the low current efficiency of Sb electrode position due to side reactions, as well as the requirement for wastewater disposal [19].

An economical and environment-friendly method is imperative for Sb extraction. In our previous work, a process of molten salt smelting [10] was adapted to smelt Sb_2S_3 directly in the molten NaCl-Na_2CO_3 system; the significant advantages of this process were low temperature and S-fixing, but high consumption of molten salt and difficulties in molten salt separation were its shortcomings. However, it was found that the direct reaction between Sb_2S_3, ZnO, and C was completed in the absence of a molten medium. Hence, it was inferred that the process entailed roasting of Sb_2S_3 with sulfur-fixing and reductant to yield Sb metal and other sulfides at low temperature, following which the solid roasted products could be separated by beneficiation. Meanwhile, Pb and Zn smelters entail the production of large quantities of secondary ZnO ash (ZnO > 70%) [20,21], which are low in value and cannot return to the hydrometallurgical process of Zn because of corrosion compositions.

Therefore, our team proposed a method of combined concentration and smelting process to extract Sb from stibnite. Firstly, stibnite was engaged in S-fixing and reduction roasting using ZnO and C as the S-fixing agent and reductant, and the products are Sb and ZnS. The roasted products were then separated by gravity and flotation to obtain Sb powder and ZnS concentrate. The prominent advantages of this new method are its low operating temperature, and the clean production and synergetic disposal of ZnO ash. This work focused on the phase and morphology transformations of Sb in the processes of S-fixing and reduction roasting. The objective of this work was to obtain a high Sb generation rate and favourable particle characteristics of Sb for the subsequent process of beneficiation, and also to provide a potential method for the extractive metallurgy of sulfide ore.

2. Experimental

2.1. Materials and Instruments

The main reagents used in the experiment were ZnO, Sb_2S_3, and C powder; C powder and ZnO were procured from Sinopharm Chemical Reagent Co., Ltd. (Shanghai, China), and Sb_2S_3 from Guangdong WengJiang Chemical Reagent Co., Ltd. All reagents used in the experiment were analytically pure. The particle size of Sb_2S_3 was 250–300 mesh. Roasting was carried out in a tubular furnace (SGMT60/12A, Sigma Furnace Industry Co., Ltd., Luoyang, China). The components of the equipment used for roasting are shown in Figure 1.

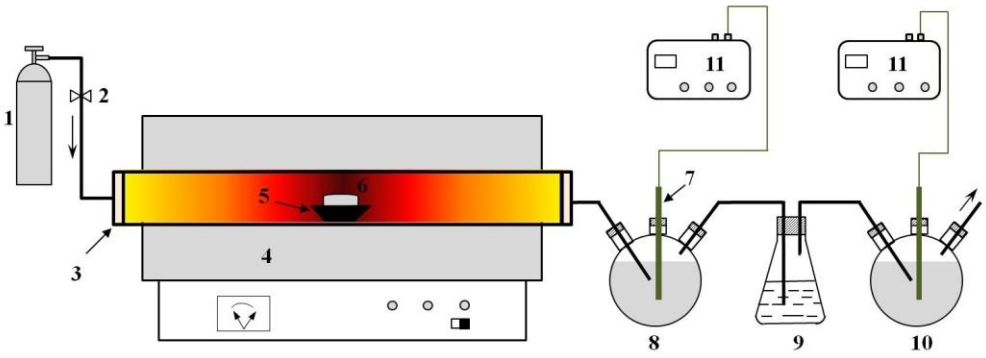

Figure 1. Component diagram of experimental equipment for roasting. 1—N_2 gas cylinder; 2—Flow meter; 3—Sealing flange; 4—Tube furnace; 5—Crucible; 6—Sample; 7—Electrode; 8—$KMnO_4$ solution; 9—Azaleine solution; 10—Na_2CO_3 solution; and 11—pH meters.

2.2. Methods

The total amount of Sb_2S_3, ZnO, and C powder used was 15 g, in the molar ratio 1:3:3. The powder was taken in a beaker, and alcohol (75 mL) was added. The beaker was then placed in an ultrasonic machine and the mixture was mechanically stirred for 30 min. The beaker was then placed in a drying oven at 60 °C. The powder was then placed in a mould and crushed into pieces after volatilisation of the alcohol. The raw material, pressed into blocks, was loaded into a crucible and roasted in the tube furnace at a certain temperature in N_2 atmosphere. The N_2 flow-rate during the trials was 2 L/min. The gas generated was successively pumped into $KMnO_4$ solution, magenta solution, and Na_2CO_3 solution to detect SO_2 generation according to Reaction (1). The pH values of the $KMnO_4$ solution were recorded every 5 min using a pH meter. The sample was withdrawn from the furnace after the setting time. The phases and morphologies of the products were measured using a Rigaku D/max 2550 VB + 18 kW X-ray powder diffractometer and a scanning electron microscope (SEM, JSM-6490LV, JEOL, Akishima, Tokyo, Japan), respectively. The phase content of Sb in the roasted products was also analysed by chemical titration (oxidation method by cerous sulfate [22])

$$2KMnO_4 + 5SO_2 + 2H_2O = 2MnSO_4 + K_2SO_4 + 2H_2SO_4 \quad (1)$$

The roasted products were dressed directly through flotation and gravity separation to obtain ZnS concentrate and Sb powder. The Sb powder can be purified by the current pyrometallurgical refining process with the addition of Na_2CO_3 and O_2 blowing. The process flow chart is shown in Figure 2. In this paper, we focused on the phase and morphology transformations in the process of S-fixing and reduction roasting of Sb_2S_3, and the separation of the roasted products was not studied in detail.

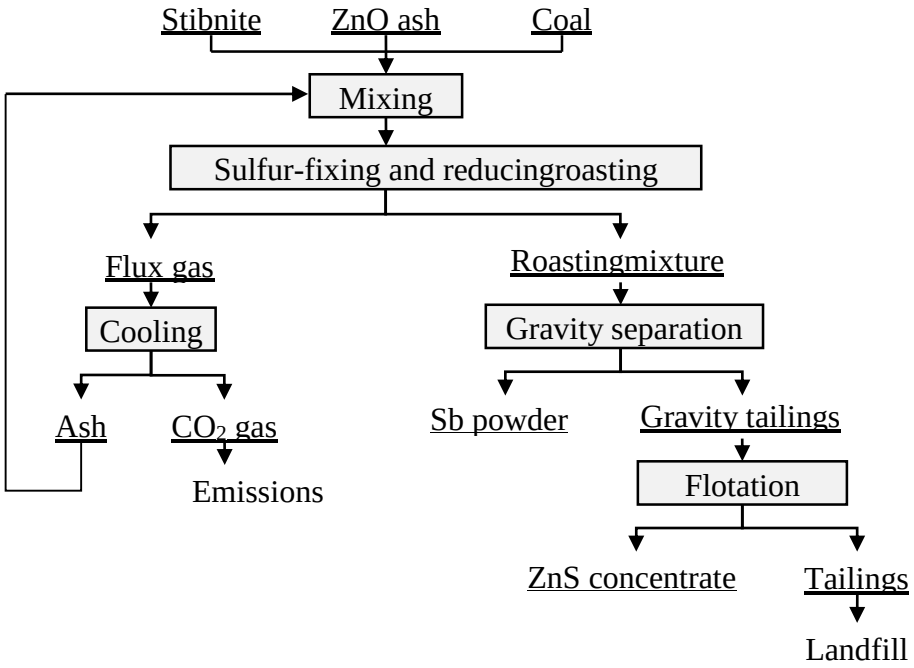

Figure 2. Process of S-fixing and reduction roasting of stibnite (Sb_2S_3).

2.3. Thermodynamic Calculations

The reactions possible during the experiment are shown in Table 1. To investigate the thermodynamic feasibility of these reactions, the HSC software was used to calculate the relationship between the Gibbs free energy (ΔG^{θ}) and temperature for each reaction, and the results are shown in Figure 3. The diagram indicates that the ΔG^{θ} values of reactions (7) and (8) are always greater than zero, while the ΔG^{θ} values of all the other reactions are less than zero in the temperature range 500–1000 °C. For the direct reducing reaction of ZnO shown in (9), the ΔG^{θ} value is also positive below 1000 °C, so the reducing reaction of ZnO cannot be carried out before 1000 °C. This result is also in agreement with standard industrial practice. With increase in temperature, the ΔG^{θ} values of Reactions (2), (3), (5) and (6) become more negative. This suggests that an increase in temperature is favourable for the direct generation of Sb and reduction of Sb_2O_3. However, the increase in temperature is less effective on Reaction (7). This indicates that, in theory, an increase in temperature can promote the reaction and facilitate the formation of Sb.

Table 1. Reactions possible during the experiment.

Reductions	No.
$Sb_2S_3 + 3ZnO + 1.5C = 2Sb + 3ZnS + 1.5CO_2(g)$	(2)
$Sb_2S_3 + 3ZnO + 3C = 2Sb + 3ZnS + 3CO(g)$	(3)
$Sb_2S_3 + 3ZnO = Sb_2O_3 + 3ZnS$	(4)
$Sb_2O_3 + 1.5C = 2Sb + 1.5CO_2(g)$	(5)
$Sb_2O_3 + 3C = 2Sb + 3CO(g)$	(6)
$Sb_2S_3 + 2Sb_2O_3 = 6Sb + 3SO_2(g)$	(7)
$ZnO + CO(g) = Zn + CO_2(g)$	(8)
$ZnO + C = Zn + CO(g)$	(9)
$C + CO_2(g) = 2CO(g)$	(10)

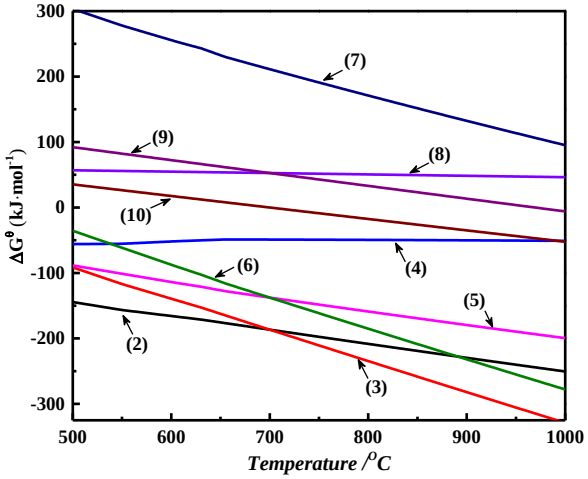

Figure 3. Relationship between ΔG^{θ} and temperature for each reaction in the system.

3. Results and Discussion

3.1. Effect of Temperature on Roasting Results

Sb_2S_3, ZnO and C powder were mixed in a molar ratio of 1:3:3. The particle size of the C powder was 150–200 mesh, and the roasting time was 2 h. The effects of roasting temperature on the Sb phase distribution and SO_2 emission were evaluated in the temperature range 600–1000 °C. The results of Sb phase distribution are shown in Figure 4a, and the changes in the pH of $KMnO_4$ solution with time are shown in Figure 4b. The pH value of the $KMnO_4$ solution reflects the generation of SO_2 during roasting.

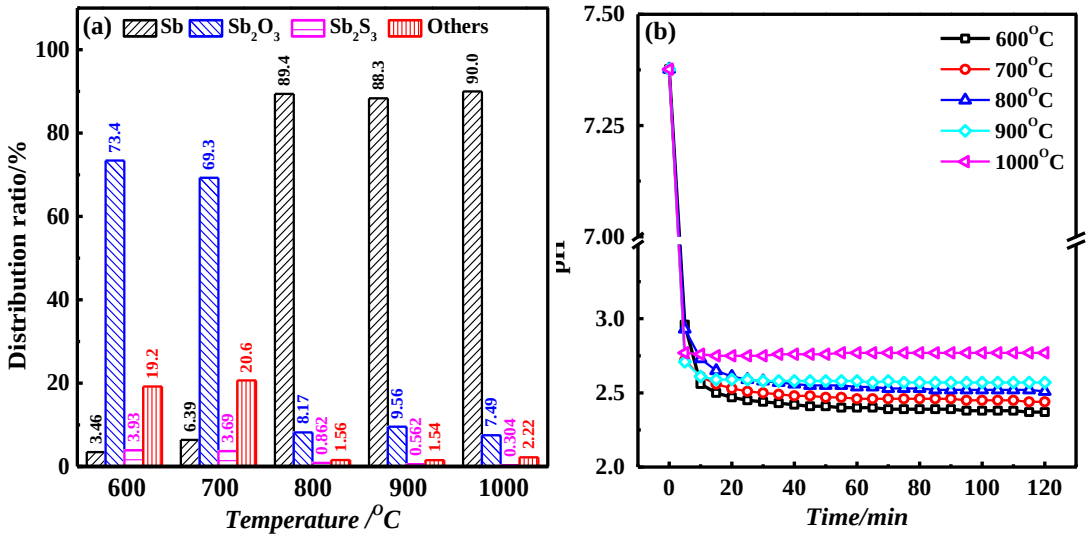

Figure 4. (**a**) Phase distribution ratios of the roasted products at different temperatures; and (**b**) pH values of the $KMnO_4$ solution.

It can be seen from Figure 4a that the main phase of Sb in the roasted products was Sb_2O_3 at temperatures lower than 800 °C and little metallic Sb was obtained. As temperature increased to 800 °C, the generation rate of metallic Sb increased sharply, and its proportion rose to 89.4%. As temperature increased further i.e., beyond 800 °C, the proportion of Sb changed negligibly. During the entire process of heating, the proportion of Sb_2S_3 decreased, indicating that the conversion reactions of Sb_2S_3 progressed adequately. The XRD patterns of the roasting products of Sb_2S_3-ZnO-C mixture at different temperature were investigated in our previous report [23], and the results proved that Sb_2O_3 and Sb

were yielded after 600 °C and 800 °C respectively, which was in very good agreement with the phase distribution results. Figure 4b shows that the pH value of the $KMnO_4$ solution at all temperatures decreased sharply in the first 5 min and then gradually stabilised. This phenomenon was likely due to the oxidisation of Sb_2S_3 to yield SO_2; the tube was exposed to air when the furnace door was opened for the reactant mixture to be loaded, and hence the pH of the solution dropped dramatically. When O_2 was depleted, the production of SO_2 ceased and the pH of the solution stabilised, thereby resulting in very little SO_2 generation in the subsequent process of roasting. However, the pH value of the $KMnO_4$ solution increased with temperature, and also achieved equilibration quickly at 1000 °C. As calculated in Figure 3, an increase in temperature can promote the sulfur-fixing and reducing reaction and facilitate the formation of Sb, and sulfur was fixed by ZnO in the form of ZnS rather than SO_2 and S^O [14]. So the pH of $KMnO_4$ solution did not decrease.

The SEM and energy-dispersive X-ray spectroscopy (EDX) analysis of the products of roasting at six temperature values are presented in Figure 5 and Table 2, respectively. As shown, large amounts of Sb_2O_3 with perfect rhomboidal dipyramid morphology were obtained at 500 °C and 600 °C. It is established in the literature [1] that Sb_2O_3 has two crystal forms, i.e., cubic and rhomboidal, and the former transforms into the latter at temperatures beyond 550 °C. Sb_2O_3 melts as temperature increases beyond 656 °C. Hence, coarse and regular Sb_2O_3 particles were observed in the temperature range 500–600 °C, whereas the roasted products presented fine particles at 700 °C, entirely devoid of Sb_2O_3 and almost mixed with ZnS. At 800 °C, metallic Sb with spherical particles were obtained as Sb has a low melting point of 630 °C and the particles grew continuously with increase in temperature. Meanwhile, pure ZnS grains with low Sb content were obtained beyond 800 °C, which indicates that the S-fixing and reduction reactions had been carried out thoroughly. Based on these findings, along with the results displayed in Figures 4 and 5, the formation of Sb can be divided into two steps. The first step is the cross-reaction between Sb_2S_3 and ZnO to obtain Sb_2O_3 and ZnS, and the second step is the reduction of Sb_2O_3 by C to Sb. Comprehensive consideration suggests that the best roasting temperature is 800 °C.

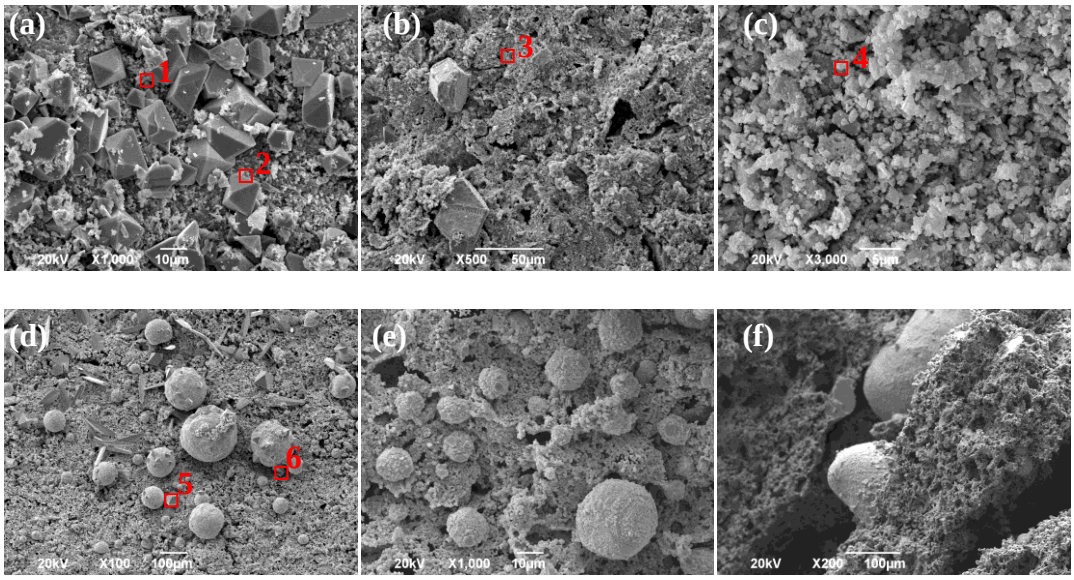

Figure 5. SEM images of the roasted products at different temperatures: (**a**) 500 °C; (**b**) 600 °C; (**c**) 700 °C; (**d**) 800 °C; (**e**) 900 °C; and (**f**) 1000 °C.

Table 2. EDS results of the elemental contents of the roasted products at the selected points (atom %).

Points	Sb	Zn	S	O
1	96.00	-	-	4.00
2	20.22	49.16	28.03	2.60
3	90.13	4.08	1.64	4.15
4	41.18	36.67	19.55	2.6
5	100	-	-	-
6	1.06	69.44	30.50	-

3.2. Effect of C Particle Size on Roasting Results

Sb_2S_3, ZnO and C powder were taken in the molar ratio 1:3:3. The roasting temperature and time were 800 °C and 2 h, respectively. The effect of the size of C powder on roasting was investigated. The phase distribution ratio of the roasted products is shown in Figure 6a, and the changes in the pH values of the $KMnO_4$ solution with time are shown in Figure 6b.

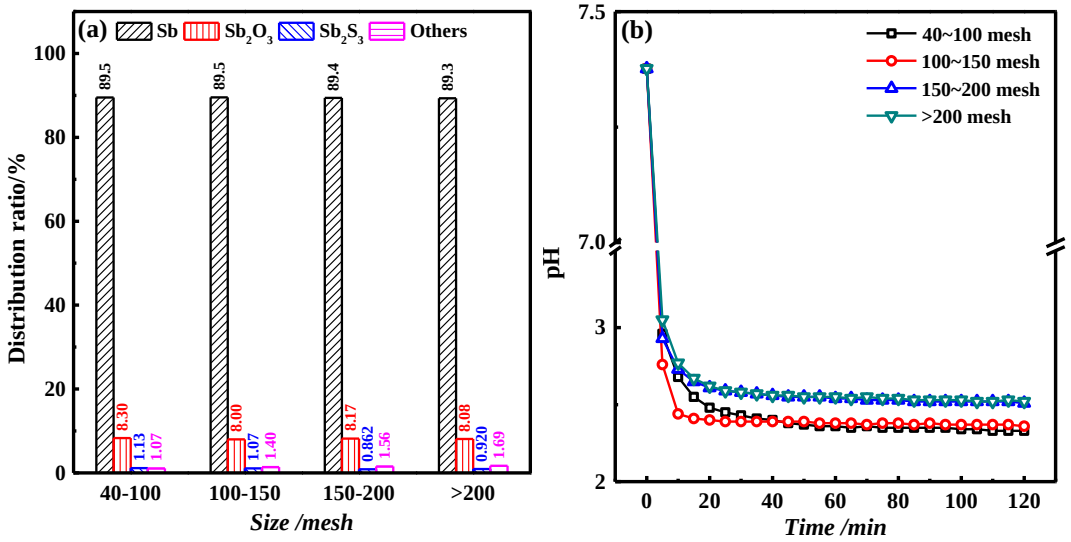

Figure 6. (**a**) Phase distribution ratio of Sb in the roasted products with different C powder sizes; and (**b**) pH values of $KMnO_4$ solution.

Figure 6a indicates that the C powder size had little effect on the phase distribution of Sb. Sb was mainly in the form of metallic Sb in the roasted products with a proportion of about 89%, followed by Sb_2O_3, which accounted for about 8% of the total Sb content. As the powder was mixed evenly and compacted into blocks, there was relatively sufficient contact among the particles, and hence the C powder size had little effect on the phase distribution of Sb. It can be seen from Figure 6b that the smaller the particle size of C powder, the higher the pH of the $KMnO_4$ solution is. This indicates that the effect of S-fixing improves with the fineness of C powder. This is because greater fineness of the particle enhances contact between reactants, thereby accelerating the reaction rate of S-fixing, reducing the emission of SO_2 and improving the effect of sulfur-fixing. However, the finer the granularity, the higher the cost. Therefore, the particle size of 100–150 mesh is the most suitable.

3.3. Effect of ZnO Content on Roasting Results

The roasting temperature and time were 800 °C (1073 K) and 2 h, respectively. The C powder particle size was 100–150 mesh. The phase distribution ratio of Sb in the roasted product and the pH value of the $KMnO_4$ solution at different content of ZnO (0.8–1.2 times the stoichiometric requirement), according to equilibrium Reaction (2), are shown in Figure 7.

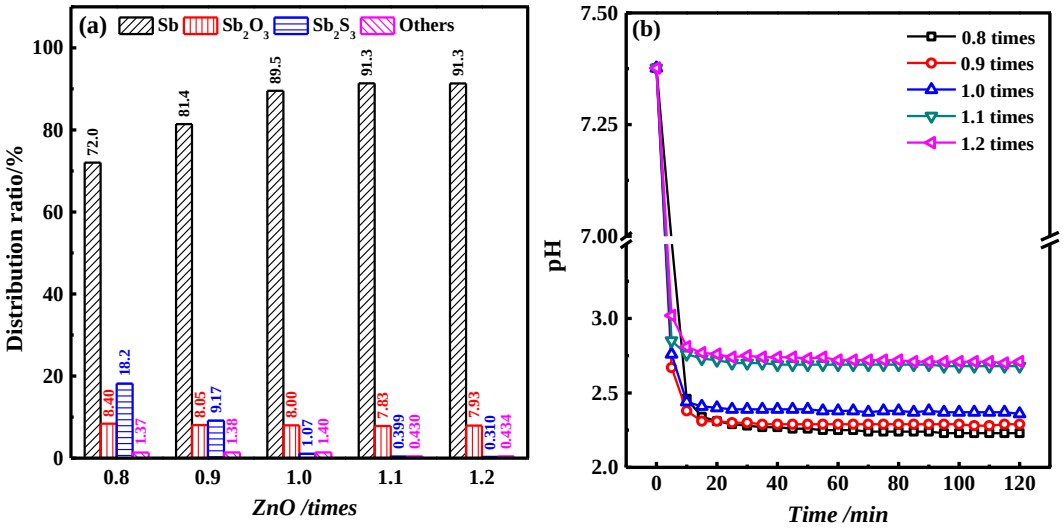

Figure 7. (**a**) Phase distribution ratio of Sb in the roasted products; and (**b**) pH value of $KMnO_4$ solution at different contents of ZnO.

Figure 7a indicates that the proportion of Sb gradually increased from 72.0% to 91.3%, while that of Sb_2S_3 decreased from 18.2% to 0.31% as the content of ZnO increased from 0.8 to 1.2 times the stoichiometric requirement. When the content of ZnO reached 1.1 times the stoichiometric requirement (α_{ZnO}), the proportion of Sb gradually stabilised, reaching 91.3%. The proportion of Sb_2O_3 changed negligibly and accounted for about 8%. As the reaction system can be described in two steps, i.e., ZnO reacts with Sb_2S_3 to generate Sb_2O_3 and ZnS, following which Sb_2O_3 reacts with C powder to generate Sb, a change in the amount of ZnO can affect the amounts of Sb_2S_3 and Sb, but not that of Sb_2O_3.

From the pH values measured, it can be seen that increasing the amount of ZnO increased the final pH of the solution after stabilisation. This shows that increasing the amount of ZnO can improve the effect of S-fixing but no significant enhancement was seen at ZnO contents greater than 1.1 times the stoichiometric requirement. As ZnO is a sulfur-fixing agent, the amount of ZnO directly affects the S-fixing effect. Therefore, the ZnO content of 1.1 times the stoichiometric requirement was selected.

3.4. Effect of Time on Roasting Results

The roasting temperature was 800 °C. The C powder particle size was 100–150 mesh and the content of ZnO was 1.1 times the stoichiometric requirement. The effects of roasting time on the phase distribution of Sb in the roasted products and the pH value of the $KMnO_4$ solution are shown in Figure 8.

Figure 8a indicates that the proportion of Sb increased gradually and that of Sb_2O_3 decreased with time. At 2 h, the reduction was nearly complete, and the proportion of Sb was 91.3%. However, as Sb is gradually reduced by volatilisation, the proportion of Sb started to decrease, and that of Sb_2O_3 started to increase after 2 h. The roasting time had little effect on the proportion of Sb_2S_3. The pH value of the $KMnO_4$ solution was mostly stable, and the roasting time had little influence on the effect of S-fixing. Therefore, the optimum roasting time was determined to be 2 h and the proportion of Sb obtained was 91.3%.

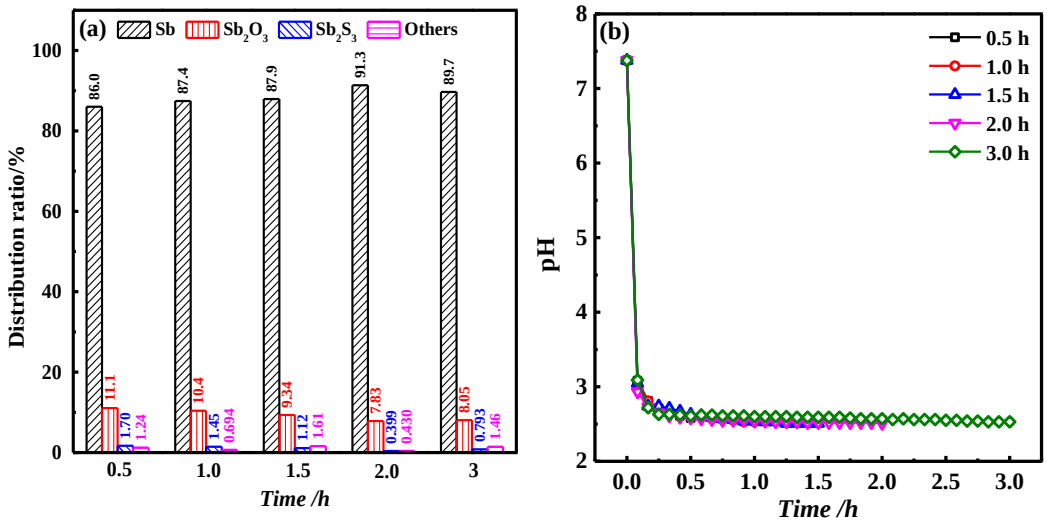

Figure 8. (**a**) Phase distribution ratio of Sb in the roasted products; and (**b**) pH value of $KMnO_4$ solution at different roasting times.

3.5. Effect of Cooling Mode on Roasting Results

To investigate the effect of the cooling mode on the crystal forms and structures of the roasted products, programmed cooling was carried out at a rate of 3 °C/min, and natural cooling was performed in the tube furnace. The SEM analysis was used to examine the product morphology. The changes in temperature during the two cooling modes, and the SEM images of the products are presented in Figures 9 and 10, respectively. As shown, in the case of the programmed cooling mode, the temperature declined linearly from 800 °C to 400 °C in 133 min. However, in the case of natural cooling, the decrease in temperature was initially rapid but progressed slowly thereafter at a rate lower than that of programmed cooling. As shown in Figure 10, large amounts of Sb particles with perfect dipyramid morphology were obtained in both the cooling modes. The Sb particles obtained in the natural cooling mode presented aggregation and were larger; recrystallisation was observed on the surface of the Sb particles, which were determined to be composed of large microcrystals. When compared with natural and splat cooling, programmed cooling yielded smooth and single-crystal Sb particles with rhombohedral crystals and homogenous distribution in the roasted mixture. However, in both the cooling modes, the Sb particles obtained were independent and had little bonding with ZnS, thereby facilitating the separation of Sb and ZnS in the subsequent process of beneficiation.

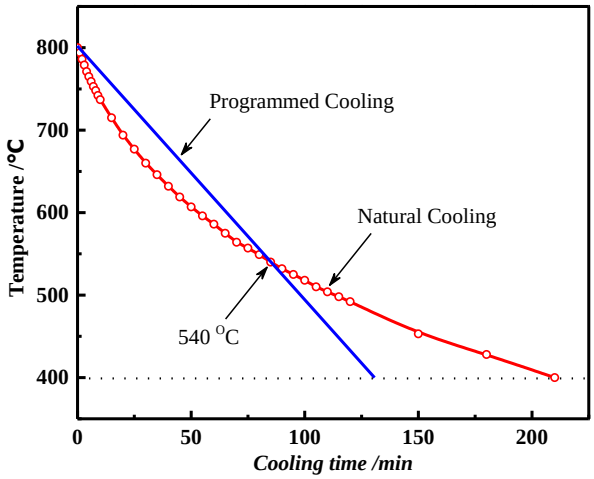

Figure 9. Cooling curves of programmed cooling and natural cooling.

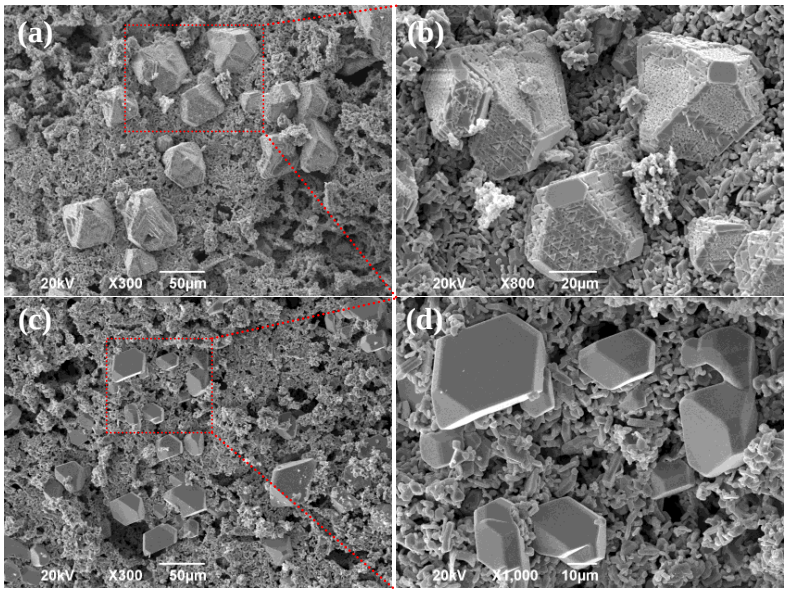

Figure 10. SEM images of the roasted products: (**a**) and (**b**) programmed cooling; and (**c**) and (**d**) natural cooling.

3.6. Energy Consumption Comparision

Through a low-temperature sulfur-fixing and reduction roasting and a gravity-flotation combined beneficiation process, metallic Sb was obtained. This represents a 200–300 °C decrease in temperature compared with the traditional process, which may reduce energy and refractory materials consumption dramatically. The economic feasibility based on energy consumption of the new process was calculated and compared with the current process in Table 3. The conventional pyrometallurgy process primary development is the blast furnace. According to the production practice [6,7], the fuel consumption of every ton of Sb in the oxidising-roasting and reduction-smelting process is as follows: coke: 906 kg, bituminous coal: 123 kg and anthracite coal: 507 kg; this resulted in 4.62 t CO_2 greenhouse gas emission. Meanwhile, the sulfur in stibnite in the form of sulfide was oxidised to SO_2, which is low in concentration and consumes large alkaline solutions to absorb. However, the fuel consumption of the new process was estimated as 1131 kg anthracite coal for every ton Sb; 37% of it is used for reduction and other 63% for combustion. The energy cost calculation of new method was based on the practice of gold ore shaking table separation and zinc concentrate flotation [24]. The energy cost of total beneficiation is low, and the total cost is 3.38 × 1010 GJ/t, which is found to be 24.9 pct lower than 4.5 × 1010 GJ/t of energy required in the conventional process. Meanwhile, the CO_2 emission decreased to 3.29 t; in particular, the SO_2 generation decreased to 0.04 t. This represents a large environmental benefit compared with the conventional process.

Table 3. The standard energy consumption to produce 1t of antimony by the current pyrometallurgy process and this metallurgy and beneficiation combined process via the present study.

The Conventional Pyrometallurgy Process		**Metallurgy and Beneficiation Combined Process**	
Unit operation	Energy cost GJ·t^{-1}	Unit operation	Energy cost GJ·t^{-1}
Oxidising-roasting	3.05 × 1010	Roasting	3.28 × 1010
Reduction-smelting	1.45 × 1010	Gravity separation	4.69 × 108
		Flotation separation	5.50 × 108
Total costing =	4.5 × 1010	Total costing =	3.38 × 1010
CO_2 emission	4.62 t	CO_2 emission	3.29 t
SO_2 generation	0.81 t	SO_2 generation	0.04 t

Calculation standard: where calorific value coke = 3 × 107 J/kg, bituminous coal = 2.7 × 107 J/kg, anthracite coal = carbon = 2.9 × 107 J/kg, S content in all fuel was 1 pct; CO_2 emitted during the consumption of fuel. Energy consumption of the gravity separation and flotation separation were 36.1 kWh/t and 60.0 kWh/t.

4. Conclusions

The thermodynamic mechanisms and experimental conditions of S-fixing and reduction roasting in the process of Sb smelting were studied. The thermodynamic analysis shows that the ΔG^{θ} value of the overall reaction of S-fixing and reduction is less than zero and that Sb_2O_3 can be reduced to Sb under the given conditions in the system. It can be inferred from the experiments that the course of the reaction can be divided into two main steps, i.e., S-fixing and reduction. The optimal reaction conditions are as follows: roasting temperature of 800 °C, carbon powder size of 100–150 mesh, content of ZnO 1.1 times the stoichiometric requirement, and roasting time of 2 h. Under these optimum conditions, the proportion of Sb, as determined from the phase distribution of Sb in the product, is 91.3%. The natural and programmed cooling modes both yielded rhombohedral Sb particles that had little bonding with ZnS, while the programmed cooling mode also yielded smooth and single-crystal Sb particles, and these were convenient for the separation of Sb and ZnS in the subsequent process of beneficiation. The proposed process is greener and has an increased economic attraction to the extraction Sb from stibnite.

Author Contributions: Z.O. carried out the experiments research and L.Y. designed the research and wrote the paper, C.T. and Y.C. reviewed and contributed to the final manuscript.

Acknowledgments: This project was supported financially by the National Nature Science Foundation of China (Grant No. 51604105) for which the authors are grateful. We also acknowledge the several helpful comments and suggestions from anonymous reviewers.

Conflicts of Interest: The authors declare no conflict of interest.

References

1. Ravinder, S.M.; Thomas, F.; George, P.D. Antimony in the metallurgical industry: A review of its chemistry and environmental stabilization options. *Hydrometallurgy* **2016**, *164*, 141–153. [CrossRef]
2. Dupont, D.; Arnout, S.; Jones, P.T.; Binnemans, K. Antimony recovery from end-of-life products and industrial process residues: A critical review. *J. Sustain. Metall.* **2016**, *2*, 79–103. [CrossRef]
3. Yang, T.Z.; Xie, B.Y.; Liu, W.F.; Zhang, D.C.; Chen, L. Enriched of gold in antimony matte by direct smelting of refractory gold concentrate. *JOM* **2018**, *70*, 1018–1023. [CrossRef]
4. Anderson, C.G. The metallurgy of antimony. *Chem. Erde-Geochem.* **2012**, *72*, 3–8. [CrossRef]
5. Yang, J.G.; Tang, C.B.; Chen, Y.M.; Tang, M.T. Separation of antimony from a stibnite concentrate through a low-temperature smelting process to eliminate SO_2 emission. *Metall. Mater. Trans. B* **2011**, *42B*, 30–36. [CrossRef]
6. Zhao, T.C. *Aantimony*, 1st ed.; Metallurgical Industry Press: Beijing, China, 1987.
7. Habashi, F. *Handbook of Extractive Metallurgy*; WILEY-VCH: Weinheim, Germany, 1997; Volume II.
8. Liu, W.; Luo, H.L.; Qing, W.Q.; Zheng, Y.X.; Yang, K.; Han, J.W. Investigation into oxygen-enriched bottom-blown stibnite and direct reduction. *Metall. Mater. Trans. B* **2014**, *45*, 1281–1290. [CrossRef]
9. Chen, M.; Dai, X. Microscopic study of the phase transformation during the oxygen-enriched direct smelting of jamesonite concentrate. *JOM* **2018**, *70*, 41–46. [CrossRef]
10. Ye, L.G.; Tang, C.B.; Chen, Y.M.; Yang, S.H.; Yang, J.G.; Zhang, W.H. One-step extraction of antimony from low-grade stibnite in sodium carbonate-sodium chloride binary molten salt. *J. Clean. Prod.* **2015**, *93*, 134–139. [CrossRef]
11. Ye, L.G.; Hu, Y.J.; Xia, Z.M.; Tang, C.B.; Chen, Y.M.; Tang, M.T. Solution behavior of ZnS and ZnO in eutectic Na_2CO_3-NaCl molten salt used for Sb smelting. *J. Cent. South. Univ.* **2017**, *24*, 1269–1274. [CrossRef]
12. Li, Y.; Chen, Y.M.; Xue, H.T.; Tang, C.B.; Yang, S.H.; Tang, M.T. One-step extraction of antimony in low temperature from stibnite concentrate using iron oxide as sulfur-fixing agent. *Metals* **2016**, *6*, 153. [CrossRef]
13. Padilla, R.; Chambi, L.C.; Ruiz, M.C. Antimony production by carbothermic reduction of stibnite in presence of lime. *J. Min. Metall. Sect. B-Metall.* **2014**, *50*, 5–13. [CrossRef]
14. Padilla, R.; Aracena, A.; Ruiz, M.C. Kinetics of stibnite (Sb_2S_3) oxidation at roasting temperatures. *J. Min. Metall. Sect. B-Metall.* **2014**, *50*, 127–132. [CrossRef]

15. Mahlangu, T.; Gudyanga, F.P.; Simbi, D.J. Reductive leaching of stibnite (Sb_2S_3) flotation concentrates using metallic iron in a hydrochloric acid medium II: Kinetics. *Hydrometallurgy* **2007**, *88*, 132–142. [CrossRef]
16. Yang, J.G.; Wu, Y.T. A hydrometallurgical process for the separation and recovery of antimony. *Hydrometallurgy* **2014**, *143*, 68–74. [CrossRef]
17. Awe, S.A.; Sundkvist, J.E.; Bolin, N.J.; Sandstrom, A. Process flow sheet development for recovering antimony from Sb-bearing copper concentrates. *Miner. Eng.* **2013**, *49*, 45–53. [CrossRef]
18. Awe, S.A.; Sandstrom, A. Selective leaching of arsenic and antimony from a tetrahedriterich complex sulphide concentrate using alkaline sulphide solution. *Miner. Eng.* **2010**, *23*, 1227–1236. [CrossRef]
19. Saleh, T.A.; Sari, A.; Tuzen, M. Effective adsorption of antimony (III) from aqueous solution by polyamide-graphene composite as a novel adsorbent. *Chem. Eng. J.* **2017**, *307*, 230–238. [CrossRef]
20. Wang, Q.M.; Guo, X.Y.; Tian, Q.H.; Jiang, T.; Chen, M.; Zhao, B.J. Effects of Matte grade on the distribution of minor elements (Pb, Zn, As, Sb, and Bi) in the bottom blown copper smelting process. *Metals* **2017**, *7*, 502. [CrossRef]
21. Zdzislaw, A.; Katarzyna, N. Environmental mobility of trace elements present in dusts emitted from Zn-Pb metallurgical processes. *Environ. Earth Sci.* **2016**, *75*, 956–961. [CrossRef]
22. Yu, L.; Fu, B. *The Analysis Handbook of Nonferrous Metallurgy*; Metallurgical Industry Press: Beijing, China, 2004.
23. Ouyang, Z.; Liu, S.F.; Tang, C.B.; Chen, Y.F.; Ye, L.G. Kinetics studies for sulfur-fixing and roasting reduction of antimony sulfide for direct antimony extraction. *Vacuum* **2019**, *159*, 358–366. [CrossRef]
24. Lu, G.W. *Handbook of Mineral Processing Designing*; Metallurgical Industry Press: Beijing, China, 2000.